Degradation of blue and red inks by Ag/AgCl photocatalyst under UV light irradiation

Hasan Daupor, and Asmat Chenea

Citation: AIP Conference Proceedings **1868**, 020009 (2017); doi: 10.1063/1.4995095
View online: http://dx.doi.org/10.1063/1.4995095
View Table of Contents: http://aip.scitation.org/toc/apc/1868/1
Published by the American Institute of Physics

Degradation of Blue and Red Inks by Ag/AgCl Photocatalyst under UV Light Irradiation

Hasan Daupor [a] and Asmat Chenea[b]

Chemistry Major, Faculty of Science Technology and Agriculture, Yala Rajabhat University
133 Thetsaban 3 Road, Tambol Sateng, Amphoe Mueang, Yala 95000, Thailand

[a]Corresponding author: hasan.d@yru.ac.th
[b]asmat.c@yru.ac.th

Abstract. Objective of this research, cubic Ag/AgCl photocatalysts with an average particle size of 500 nm has been successfully synthesized via a modified precipitation reaction between $ZrCl_4$ and $AgNO_3$. Method for analysis, the crystal structure of the product was characterized by X-ray powder diffraction (XRD). The morphology and composition were studied by scanning electron microscopy (SEM), Fourier transform infrared spectroscopy (FTIR), UV-vis diffuse-reflection spectra (DRS) and so on. The result showed that the optical absorption spectrum exhibited strong absorption in the visible region around 500-600 nm due to surface plasmon resonance (SPR) of metallic silver nanoparticles. SEM micrographs showed that the obtained Ag/AgCl had cubic morphology and appeared on the porous surface as the cubic cage morphology. As a result, this porous surface also positively affected the photocatalytic reaction. The photocatalytic activity of the obtained product was evaluated by the photodegradation of blue and red ink solutions under UV light irradiation, and it was interestingly, discovered that AgCl could degrade 0.25% and 0.10% in 7 hours for blue and red inks solution respectively, Which were higher than of commercial AgCl. The result suggested that the morphology of Ag/AgCl strongly affected their photocatalytic activities. O_2^-, OH^- radicals and Cl^o atom are main species during photocatalytic reaction.

INTRODUCTION

Semiconductor photocatalyst absorbs incident photons with energy higher than its band gap to transfer the light energy into chemically useful charge carriers, sub-sequently driving redox reactions at the surface of photocatalyst.Undoubtedly, the light harvesting of photocatalysts that directly dominates the generation of active redox charge carriers is a critical issue for manipulating the photocatalytic performance. The semiconductor such as TiO_2, ZnO and AgCl with considerable photoreactivity and photostability are the most extensively used materials in semiconductor photocatalysis [1].

AgCl is a photosensitive semiconductor material with an indirect band gap of 3.3 eV, which accordingly has its intrinsic light response located within the UV region. Ag/AgCl known as a new visible light plasmonic photocatalyst has attracted a considerable attention because of the localized surface plasmon resonance (LSPR) of noble metal nanoparticles [2]. Recently, Ag/gCl photocatalysts with various structures including microrods, irregular balls, hollow spheres, porous nanocomposites, cube-like, near-spherical, and boehmite-doped nanocube have been successfully synthesized [3].

Pen inks consist of complex systems, the most important component is the coloring material which comes in the form of dyes, pigments, or their combination. Dyes are soluble in the liquid body of the ink which is also known as the vehicle. On the other hand, pigments are finely ground multimolecular granules that are insoluble in the vehicle. The vehicle can consist of oils, solvents, and resins whose composition affects the flowing and drying characteristics of the ink [4].

The 4th International Conference on Research, Implementation, and Education of Mathematics and Science (4th ICRIEMS)
AIP Conf. Proc. 1868, 020009-1–020009-8; doi: 10.1063/1.4995095
Published by AIP Publishing. 978-0-7354-1548-5/$30.00

Therefore, we report a preparation method to synthesize cubic Ag/AgCl crystals by using vinyl acetate monomer as controlling agent, and apply them in photocatalytic activity of blue and red inks solution under UV light irradiation and compared with commercial AgCl.

EXPERIMENTAL

Preparation of cubic Ag/AgCl

Cubic Ag/AgCl was synthesized by the modified precipitation method. In a typical procedure, 15 g of anhydrous $ZrCl_4$ was prepared in 50 mL of deionized water and placed in a water bath (at room temperature) to help dissipate heat during dissolution. To this solution, 15 mL of vinyl acetate monomer (VAM) was added and transferred to a 250 mL three-necked flask to reflux for 30 min at 70 ºC. $AgNO_3$ solution was prepared in advance by dissolving $AgNO_3$ 5 g in diluted ammonium hydroxide solution 240 mL and transferred to reflux for 2 h at 100 ºC. After which, $AgNO_3$ aqueous solution was injected into $ZrCl_4$ solution under stirring and white dispersion was formed immediately. Subsequently, $AgNO_3$solution was poured into the $ZrCl_4$ dispersion and the mixture wasvigorously stirred for 30 min. At the end of the reaction, the product was washed thoroughly with ethanol and DI water to remove VAM. After drying at 40 ºC for about 6 h, the powder of cubic Ag/AgCl was obtained.

Sample Characterization

The morphology and crystalline structure of the samples were examined by a scanning electron microscope (SEM, Quanta 400, FEI). The phase constitution of the samples was characterized by X-ray diffraction (XRD) using a Philips PW 3710 powder diffractometer (PHILIPS X'Pert MPD, The Netherlands), Cu K_a (Ni filtered) radiation λ=1.5406 Å. The diffractograms were recorded in the 2θ range of 5-90º with a 2θ step of 0.05º and a step time of 1 s.

The diffused reflectance spectra (DRS) were measured by a UV 2401 spectrometer (Shimadzu, Japan) over the range of 200-800 nm using $BaSO_4$ as the reflectance standard material.

Evaluation of Photocatalytic Activity

Blue and red inks were chosen as the target organic compound in this study. The batch experiments were conducted with 0.1 g of respective photocatalyst suspended in 100 mL of blue and red inks solution (0.25% and 0.1%, respectively). The solution was pre-stirred vigorously in the dark for 1 hour to establish adsorption-desorption equilibrium, during the degradation, the mixture was stirred continuously by means of a magnetic stirrer. The zero time readings were then taken and the solution was irradiated. An aliquot (4 mL) was taken at time intervals and centrifuged (4500 rpm for 5 min) to remove the dispersed powder from the solution prior to the absorbance measurements. The degradation activity of blue and red ink was followed by measuring absorbance at 600 and 517 nm, respectively, using a UV–visible spectrophotometer (JASCO 6800).

RESULTS AND DISCUSSION

Morphology

The typical SEM images of as-prepared Ag/AgClphotocatalyst were presented in Figure 1. It could be clearly seen that the synthesized Ag/AgCl sample possessed uniform and cubic morphology with a length of 500 nm. In addition, the surface of some particles appeared on the porous surface as same as cubic cage morphology as reported by Tang and co-worker in 2013 [5]. Demonstrated the concentration of Cl^- ions was suitably controlled and enough, turning the crystal morphology and surface exposure to the (100) surface [6]. As a result, the surface energy of the (100) surface was lower than those of the (110) and (111) surfaces. Therefore, the growth of AgCl nuclei along the ⟨100⟩ direction will be restricted, leading to the preservation of {100} facets and the formation of {100}-facet exposed.

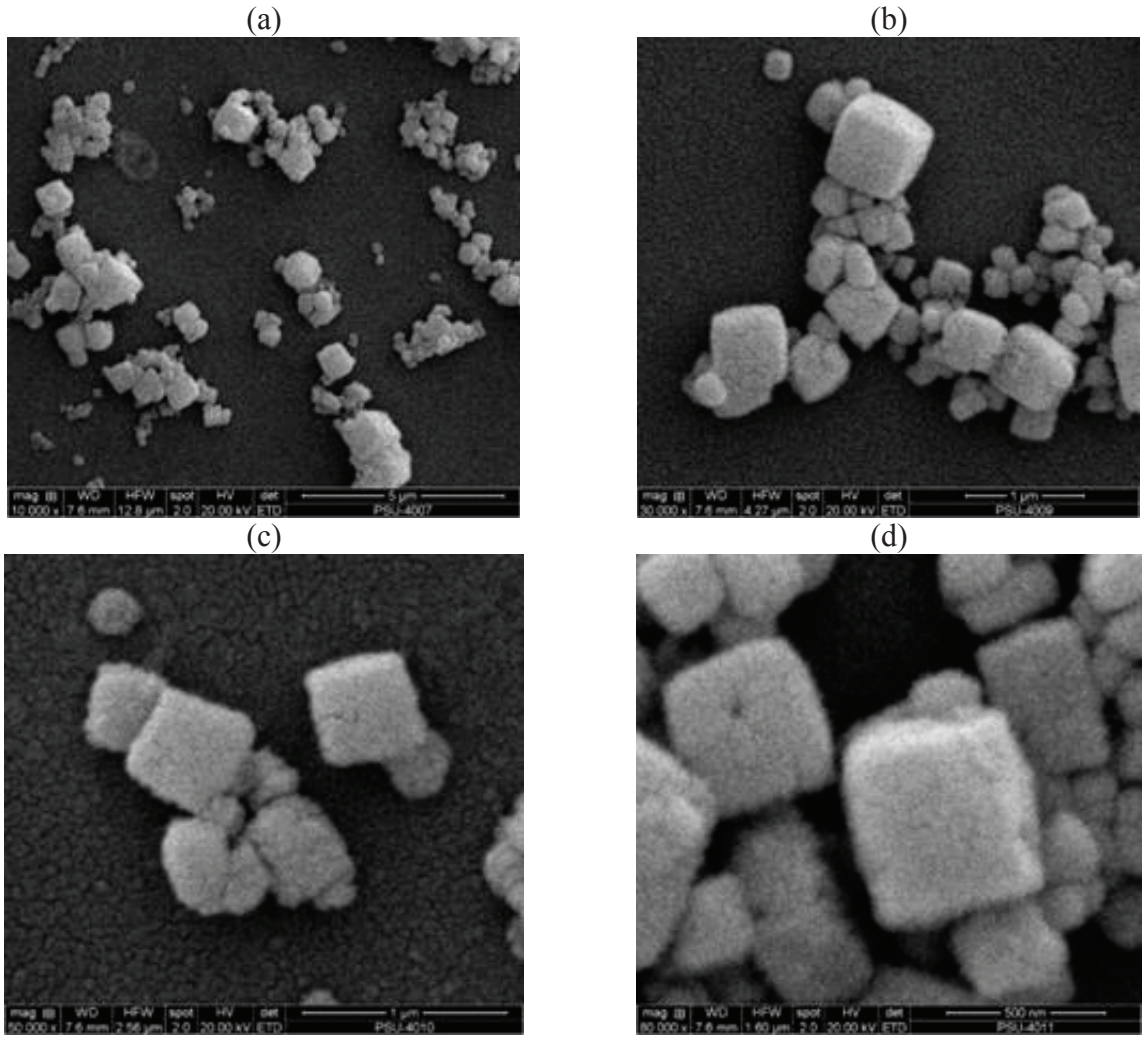

FIGURE 1. SEM images of cubic Ag/AgCl samples with different magnification

The Powder X-Ray Diffaction

Ag/AgCl particles were characterized using X-ray diffractometer (PHILIPS X'Pert MPD, The Netherlands) with Cu-Kα (Ni filtered) radiation $\lambda = 1.5406\ \text{Å}$operated at a voltage of 40 kV in the scan range of 5 to 90 degree with a 2θ of 0.05° and step time of 1 s. As shown in Figure 2. The characteristic XRD peaks at 27.8°, 32.2°, 46.2°, 54.9°, 57.6°, 67.4°, 74.5° and 76.7° were attributed to planes (111), (200), (220), (311), (222), (400), (331), and (420) of cubic phase of AgCl crystal (JCPDS No. 31-1238). No other characteristic peaks could be attributed to impurities which indicated the high purity of Ag/AgCl. The strong and narrow diffraction peaks reveal the highly crystalline [7].

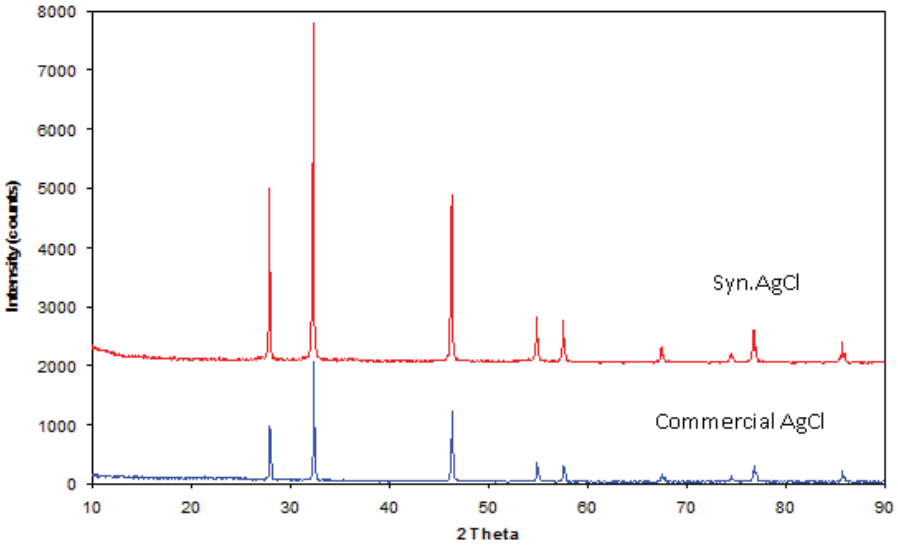

FIGURE 2. XRD pattern of synthesized Ag/AgCl (cubic Ag/AgCl) and commercial AgCl

Optical Properties

Metallic Ag nanoparticles on the AgCl surface are able to absorb light in the visible range due to the absorption properties of surface plasmon resonance (SPR) [8]. This absorption behavior corresponded with the observation reported by other researchers that it was originated from the characteristic absorption of surface plasmon resonance (SPR) of metallic Ag on the AgCl surface [9]. In figure 3, the sample of cubic Ag/AgCl possesses two absorption peaks about 500 and 600 nm, which was attributed to the relatively large sizes of these crystals. Meanwhile, the samples of commercial Ag/AgCl have no absorption peak because of pure AgCl particle.

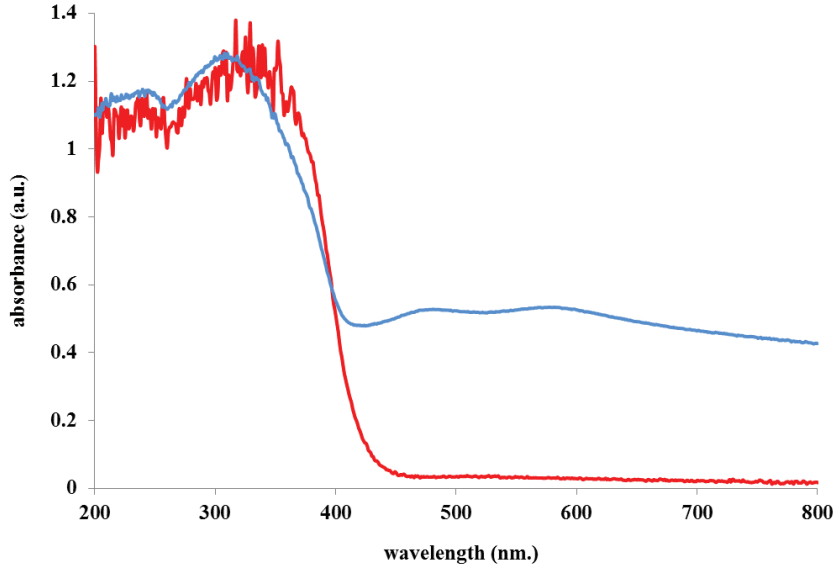

FIGURE 3. DRS spectra of cubic Ag/AgCl (blue line) and commercial AgCl (red line)

The energy band gaps of different samples are calculated based on the optical absorption edge obtained from UV-vis DRS spectra by the Kubelka-Munk equation [10]:

$$Rhv = A\left(hv - E_g\right)^{n/2} \quad (1)$$

According to Eq. (1), the estimated indirect band gap energiesof cubic Ag/AgCl is 2.80, this value agrees well with the reported band gap energy for AgCl [11]. The investigated AgCl crystals showed a narrower band gap than that of the commercial AgCl crystals at 3.25 eV [12].

(a)

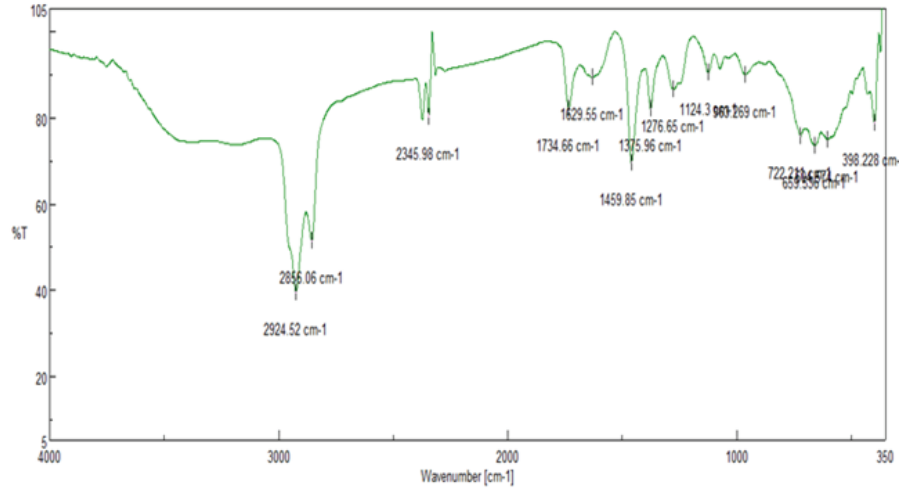

(b)

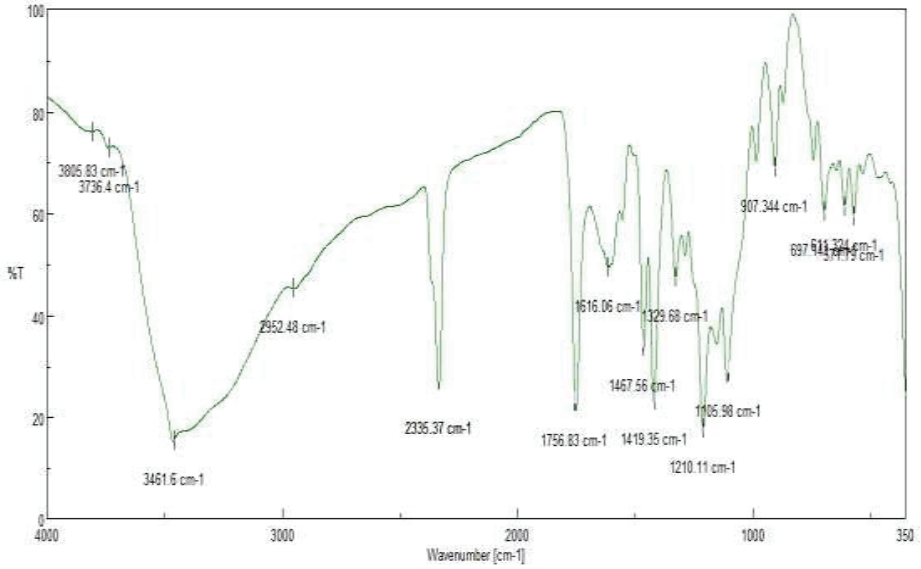

FIGURE 4. Infrared spectrum of cubic Ag/AgCl (a) and ink sample (b)

Infrared Spectrum

Fourier transform infrared spectroscopy (FTIR) was employed to analyze the chemical bonding and composition of the as-prepared samples. As shown in Figure 4a, cubic Ag/AgCl samples showed the bands at 2924 cm^{-1} and 2856 cm^{-1}assigned to C–H stretching of alkyl chain indicating the presence of vinyl acetate monomer as capping agent with the Ag/AgCl particles [13]. The peak noted at 1734 cm^{-1} was due to the stretching vibration of CO_2^- (carboxylate ion) group. The band at around 1459 cm^{-1} was ascribed to the hydroxyl group deformation vibration [14]. The peak observed below 700 cm^{-1} could be ascribed to the Ag—Cl stretching vibration.

FT-IR spectroscopy is also a technique that can be used to analyze noncolorant components found in writing inks. As shown in Figure 4b, both blue and red inks displayed the peaks at 1210 cm^{-1} originated by epoxy resins. Also, doublets were located at about 700 and 1467 cm^{-1} that were ascribed to the presence of solvents such as styrene or benzyl alcohol. Ethylene glycol contributed with quite broad peaks between 907 and 1105 cm^{-1}. A band at 1756 cm^{-1}, indicative of the presence of acids or esters [15, 16].

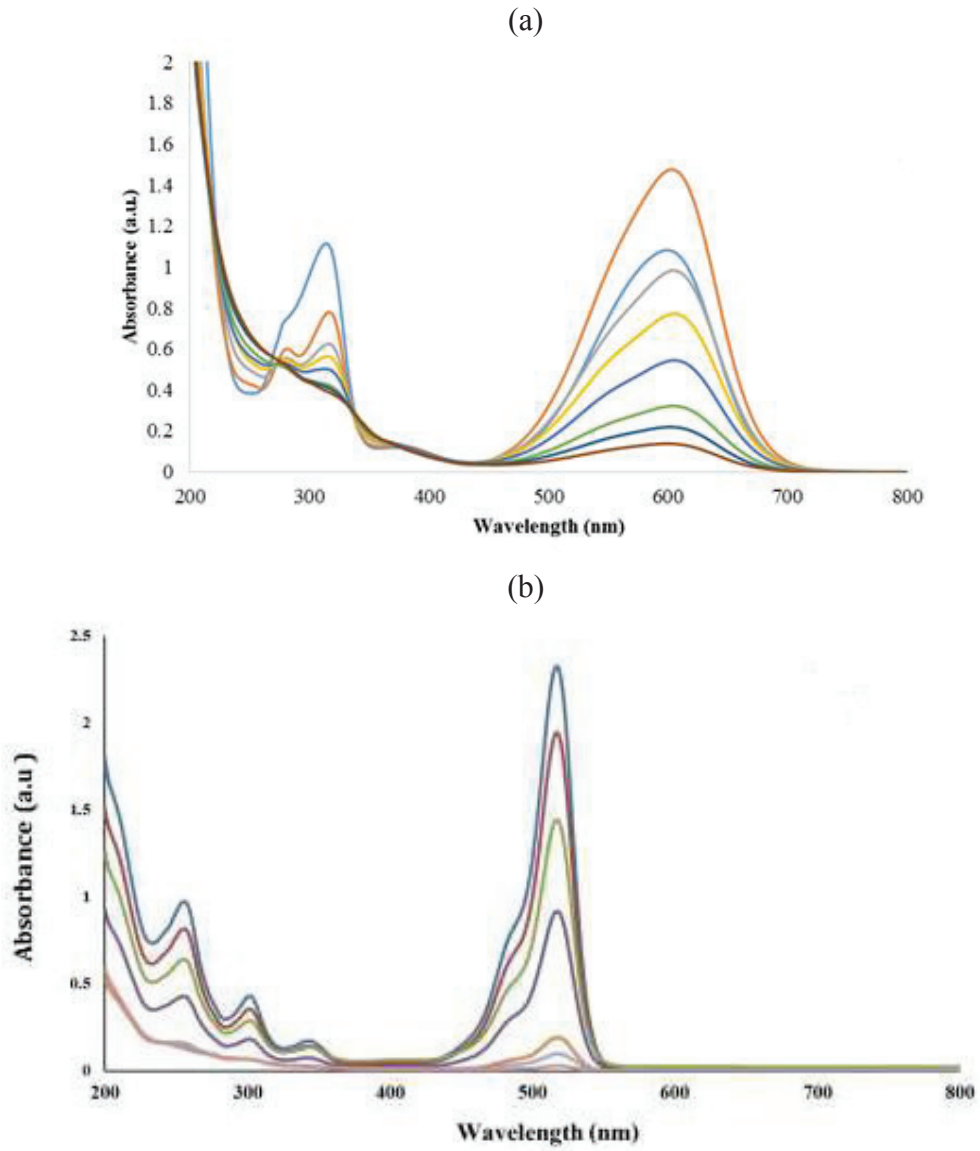

FIGURE 5. absorption decrease of blue ink solution (a) and red ink solution (b)

Photocatalytic Activity

The photocatalytic activity of the Ag/AgCl cube was evaluated by the degradation of blue and red inks under UV light irradiation. Figure 5 showed the UV–vis absorption spectra of blue and red inks aqueous solution after UV light irradiation for 7 hours in the presence of Ag/AgCl cube. The peak intensity at 600 and 517 nm represents the concentration of blue (0.25%) and red ink solution (0.1%) as shown in Figure 5a and 5b, respectively. Some of dye concentration decreased of the peak intensity before irradiation reflects the extent of adsorption of both ink on Ag/AgCl cube in the dark. It decreased markedly with extending irradiation time and almost disappears after 7 hours irradiation, suggesting the excellent photocatalytic activity of Ag/AgCl cube. For comparison, we also conducted blue and red inks photodegradation experiments with commercial Ag/AgCl under similar condition. We found the photocatalyticactivity of cubic Ag/AgCl to be much higher than that of commercial AgCl.

Possible Photocatalytic Mechanism

To understand the mechanism of the photocatalytic oxidation process thoroughly, according to the previous researches, when AgCl absorbs photons from UV light with energy equal or greater than its band gap (3.25 eV), electrons in the valence band can be excited and jump up into the conduction band leaving behind a hole in the valence band (Eq. (2)). The electron-hole pairs may recombine (Eq. (3)), or electron and hole may separate and finally be trapped as reduced Ag atom (Ag^0) (Eq. (4)), or Cl^0 atom (Eq. (6)). In general, the photogenerated electrons may also be trapped by O_2 in the solution to form superoxide ions (O_2^-) (Eq. (4)) which further transform to other reactive oxygen species. These active species also would degrade the dye molecules [17]. Despite this competing electron trapping reaction, however, the presence of metallic Ag atoms seem to indicate that the trapping of free electron by Ag^+ ions (Eq. (4)) located within the matrix may be the more favorable route. While the left over holes diffuse into the AgCl matrix to oxidize Cl^- ions to Cl atoms (Eq. (6)) which are very reactive for oxidizing species in the surrounding solution (Eq. (8)) [18]. The hole may also oxidize the adsorbed OH^- at the interface to the powerful $^{\bullet}OH$ radical (Eq. (7)) which subsequently would undergo the dye degradation as well.

$$AgCl \xrightarrow{hv} AgCl + h^+ + e^- \quad (2)$$

$$h^+ + e^- \rightarrow kT \quad (3)$$

$$Ag^+ + e^- \rightarrow Ag^0 \quad (4)$$

$$O_2 + e^- \rightarrow O_2^- \quad (5)$$

$$Cl^- + h^+ \rightarrow Cl^0 \quad (6)$$

$$OH^- + h^+ \rightarrow OH^{\bullet} \quad (7)$$

$$Cl^0 + dyes \rightarrow CO_2 + H_2O + Cl^- \quad (8)$$

$$OH^{\bullet} + dye \rightarrow CO_2 + H_2O \quad (9)$$

Under visible light irradiation, Ag metal nanoparticles absorb a photon from the visible light irradiation through the intrinsic SPR effect leading to electron-hole separation (Eq. (10)) [8, 19].

$$hv \xrightarrow{SPR\ (Ag^0)} e^-(electron) + h^+(hole) \quad (10)$$

CONCLUSION

In summary, a method to fabricate cubic Ag/AgCl via a reaction between $ZrCl_4$ and $AgNO_3$ solution. The structure formations of cubic Ag/AgCl were monitored, which revealed the growth of AgCl along the ⟨100⟩ direction will be restricted, leading to the preservation of {100} facets and the formation of {100}-facet exposed. As for the photocatalysis characteristics, cubic Ag/AgCl exhibited a considerably high catalysis activity for the decomposition of inks. It is believed that cubic Ag/AgCl composed of six thin-walled squares where both the inner and outer surfaces of the cages were accessible. It attained a large specific surface area for the heterogeneous photocatalytic reactions.

ACKNOWLEGMENT

Some parts of this work were supported by Yala Rajabhat University grant for the financial support under grant number 014/2017.

REFERENCES

1. Z. Feng, J. Yu, D. Sun, and T. Wang, *J. Colloid Interf. Sci.*, **480**, 184–190, (2016).
2. L. Han, P. Wang, C. Zhu, Y. Zhai, and S. Dong, *Nanoscale*, **3**, (7), 2931–2935, (2011).
3. H. Chen, L. Xiao, and J. Huang, *Mater. Res. Bull.*, **57**, 35–40, (2014).
4. C. D. Adam, S. L. Sherratt, and V. L. Zholobenko, *forensic Sci. Int.*, **174**, 16–25, (2008).
5. Y. Tang. Z. Jiang, G. Xing, A. Li, P. D. Kanhere, Y. Zhang, T. C. Sum, S. Li, X. Chen, Z. Dong, Z. Chen, *Adv. Funct. Mater.*, **23** (23), 2932–2940, (2013).
6. R. Dong, B. Tian, C. Zeng, T. Li, T. Wang, and J. Zhang, *J. Phys. Chem. C*, **4**, 213–220, (2012).
7. P. Wang, B. Huang, Z. Lou, X. Zhang, X. Qin, Y. Dai, Z. Zheng, and X. Wang, *Eur. J. Inorg. Chem*., **16** (2), 538–544, (2010).
8. H. Xu, H. Li, J. Xia, S. Yin, Z. Luo, L. Liu, and L. Xu, *ACS Appl. Mater. Inter.*, **3** (1), 22–29, (2011).
9. Q. Zhang, J. Ge, T. Pham, J. Goebl, Y. Hu, and Z. Lu, Y. Yin, *Angew. Chem. Int. Ed.*, **48**, (19), 3516-3519, (2009).
10. J. Cao, B. Xu, B. Luo, H. Lin, and S. Chen, *Appl. Surf. Sci.*, **257** (16) 7083–7089, (2011).
11. J. Hu, N. Jia, J.-X. Jiang, M.-G. Ma, J.-F. Zhu, R.-C. Sun, J.-Z. Li, *Mater. Lett.*, **65** (11), 1531–1534, (2011).
12. P. Wang, T. Ming, G. Wang, X. Wang, H. Yu, and J. Yu, *J. Mol. Catal. A Chem.*, **381**, 114–119, (2014).
13. I. Aiad, M. M. El-sukkary, E. A. Soliman, M. Y. El-awady, and S. M. Shaban, *J. Ind. Eng. Chem.*, **20** (5), 3430–3439, (2014).
14. X. Zhao, Y. Xia, Q. Li, X. Ma, and F. Quan, *Colloids Surfaces A*, **444**, 180–188, (2014).
15. J. Wang, G. Luo, S. Sun, Z. Wang, and Y. Wang, *J. Forensic Sci.*, **46** (5), 1093–1097, (2001).
16. J. Zie and M. Kunicki, *Forensic Sci. Int.*, **158**, 164–172, (2006).
17. J. Jiang and L. Zhang, *Chem. Eur. J*, **17** (13) 3710–3717, (2011).
18. L. Dong, D. Liang, and R. Gong, *Eur. J. Inorg. Chem.* **2012** (19), 3200–3208, (2012).
19. G. Calzaferri, M. Lanz, and D. Schu, *J. Photoch. Photobio. A*, **120**, 105–117, (1999).